



Structural Variations Induced by Temperature Changes in Rotavirus VP6 Protein Immersed in an Electric Field and Their Effects on Epitopes of The Region 300-396

C. Peña-Negrete¹, M.A. Fuentes-Acosta¹, J. Mulia¹, L.A. Mandujano-Rosas² and D. Osorio-González^{1*}

¹Molecular Biophysics Laboratory of the Faculty of Sciences, Autonomous University of the State of Mexico, Mexico

²Molecular Biophysics Modeling and Prototyping Laboratory, Mexiquense University, S. C., State of Mexico, Mexico

*Email: dog@uaemex.mx

ARTICLE INFORMATION

Received: October 10, 2019
Accepted: January 21, 2020
Published online: February 28, 2020

Keywords:

Rotavirus, VP6, Antigenic determinants

ABSTRACT

Rotavirus diarrhea is an infectious intestinal disease that causes about 215 thousand deaths annually in infants under five years old. This virus is formed by three layers of concentric proteins that envelop its genome, from which VP6 structural protein is the most conserved among rotavirus serotypes and an excellent vaccine candidate. Recent studies have shown that structural proteins are susceptible to losing their biological function when their conformation is modified by moderate temperature increments, and in the case of VP6, its antigen efficiency decreases. We performed an *in silico* analysis to identify the structural variations in the epitopes 301-315, 357-366, and 376-384 of the rotavirus VP6 protein -in a hydrated medium- when the temperature is increased from 310 K to 322 K. In the latter state, we applied an electric field equivalent to a low energy laser pulse and calculated the fluctuations per amino acid residue. We identified that the region 301-315 has greater flexibility and density of negative electrical charge; nevertheless, at 322 K it experiences a sudden change of secondary structure that could decrease its efficiency as an antigenic determinant. The applied electric field induces electrical neutrality in the region 357-366, whereas in 376-384 inverts the charge, implying that temperature changes in the range 310 K-322 K are a factor that promotes thermoelectric effects in the VP6 protein epitopes in the region 300-396.

DOI: [10.15415/jnp2020.72024](https://doi.org/10.15415/jnp2020.72024)



1. Introduction

Rotavirus is the most important etiological agent in severe diarrhea, causing about 215 thousand deaths annually in infants under five years old [1]. It is composed of 11 double-stranded ARN segments, which codify for six structural proteins (VP1-4,6 and 7) and six non-structural (NSP1-6) [2]. VP6 protein is the most immunogenic and conserved among serotypes, therefore it is speculated that it may be an excellent candidate for highly heterotypic vaccines [3]; furthermore, VP6 has been proven to induce significant protection in mice after a challenge against rotavirus, regardless of the route of administration [4]. X-ray crystallography studies with a resolution of 2-2.6 Å show that VP6 is a 95 Å long protein with a tower shape, constituted by three subunits grouped around a triple-fold central axis where contact zones are relatively charged. In the center of this trimeric molecule, there is a Zn²⁺ ion, important for stability, coordinated tetrahedrally by the His153 of each subunit; and a Cl⁻ ion, coordinated by Lys154, that compensates for the accumulation of positive charges on the axis. When folded, two domains are shown: (1) domain B, comprising amino acid residues from 335 to

397 of the C-terminus, and 150 residues of the N-terminus, and (2) domain H, which is composed of residues 151 to 334, has multiple loops and a three-layer structure that allows it to interact with the other rotavirus proteins [5-7].

An interesting feature of VP6 is its behavior as conducting material that allows charge transfer processes and metal electrodeposition [8]. Moreover, it is structurally polymorphic since it forms tubular particles (100 nm in diameter) at pH 5.0-9.0, spherical particles (45 nm in diameter) at pH 4.0, and sheets in pH changes from 6.0 to 4.0 [9-10]. These and other structural changes are associated with variations in physicochemical parameters, mainly pH and temperature, which cause differences in efficiency and stability during assembly [11-14].

An epitope or antigenic determinant refers to an antigen target zone to which an antibody specifically binds. VP6 has several groups of highly conserved reactive epitopes, mainly in the 197-397 region; they induce the immune response through CD4 T cells and CD8 T cells, which produces antiviral cytokines (IFN- γ , TNF) [15-16]. In the region 300-396, at least three epitopes of biological importance have been described: 301-315, 357-366, and 376-384 [17-18].

In the present work, we performed an *in silico* study to analyze the structural variations of VP6 when temperature changes are induced, and the protein is subjected to an electric field equivalent to an infrared laser pulse with a wavelength of 3.0 μm . We used two force fields to model the energetic interactions, then calculated and compared the fluctuations of the residues in three epitopes of VP6 located in the region 300-396. We described the charge distribution in the regions mentioned above and analyzed the implications of thermoelectric effects on their biological function.

2. Methods

2.1 Molecular Dynamics

We used Classical Molecular Dynamics to simulate the wild-type VP6 protein from its experimentally determined spatial configuration by X-ray diffraction with a resolution of 1.95 \AA (RSBS Protein Data Bank ID 1QHD). For this purpose, we used GROMACS 5.1.2 programs suite with the Gromos96 43 a force field. The protein was solvated with 47,456 water molecules with the TIP3P model inside a simulation box with rhombic dodecahedral geometry, and incorporating periodic boundary conditions. In order to keep the system neutral, Na^+ and Cl^- ions were added at a concentration of 0.15 mol/L. An NVT (number of particles, volume, and temperature are kept constant) statistical ensemble was used while controlling the temperature with the Berendsen thermostat. The cutoff radius of Van der Waals was set at 16 \AA , while Coulomb's was set at 12 \AA . The system energy was minimized using the steepest descent method. After the minimization, the simulation was carried out in three stages: i) System Relaxation, ii) equilibration, and iii) production. The energetic stability of the system was achieved before 30ns; for this reason, the production stage was carried out for 100 ns.

2.2 Structural Properties

Root mean square fluctuation per amino acid residue was calculated by

$$RMSF(i) = \left[\frac{1}{T} \sum_{t_1=1}^T r_i(t_1) - r_i(t_2) \right]^2 \Bigg|^{1/2}$$

Where $r_i(t_1)$ is the initial position of the atom i at time while $r_i(t_2)$ is its position at a later time t_2

The protein contact map provides a bidimensional representation that is invariant to rotations and translations. It is generated by a binary matrix whose entries represent the distance between all amino acid residue pairs of the protein,

that is: for two residues i and j , the input (i,j) is 1 if its distance is less than a specific limit, and otherwise is 0.

Using molecular simulation dynamics, we generated the trajectories of all the atoms of the hydrated protein complex by solving motion Newton's equations from a proposed potential energy model. The initial atom velocities were obtained randomly from a Boltzmann distribution, and the initial positions were contained in the PDB file, generated by X-ray diffraction. For those mentioned above, we obtained system configurations every 10ps, which allowed us to identify the variations of the secondary and tertiary structure of VP6 as a function of time. We identified six types of secondary structures in the protein and classified each amino acid residue during the entire production stage.

2.3 Electric Field Model

The hydrated VP6 protein was stimulated with a time-dependent pulsed electric field with a maximum at t_0 and a width σ given by

$$E(t) = E_0 \exp \left[-\frac{(t-t_0)^2}{2\sigma^2} \right] \cos[\omega(t-t_0)]$$

Where E_0 is the initial pulse amplitude whose angular frequency is in terms of the wavelength λ and the speed of light c , and is calculated using $\omega = \frac{2\pi c}{\lambda}$. In our case, the initial temperatures for the complex were set at $T = 310K$, $317K$ and $322K$ the structural variations induced by the electric field were observed with $E_0 = 1.0Vnm^{-1}$, $\sigma = 1ps$, and $\lambda = 3.0\mu m$.

Since $\lambda > 150nm$, ionization effects do not occur [19]; additionally, at room temperature, the vibrations of the water molecules and VP6 are comparable with kT . Likewise, quantum effects were not considered because they demand a considerable amount of computational resources; however, the method includes quantum corrections using forces autocorrelation functions [20].

3. Results and Discussion

Proteins are complex systems whose internal mechanics are fundamental to all cellular processes of living organisms. The coordinated movements of its amino acids residues under the force field that restricts them, link the protein structure with its biological function. For this reason, it is not a surprise that, when stimulating a protein with an external electric field, conformational changes of its entire structure are observed in nanosecond time scales that are consistent with the local and allosteric changes naturally

induced by the union of a ligand [21]. Since it is in our interest to analyze the epitopes of VP6 found in the region

300-396, Table 1 summarizes those that have been reported in the literature as a result of experimental work.

Table 1: Epitopes from the region 300-396 of VP6.

Epitope	Amino acid sequence	Biological importance	Reference
A 301-315	TPAVAALFPNAQPFE	Recognized by CD4 T cells that produce antiviral cytokines (IFN- γ). It is of such importance that this epitope is included in the RotaTeq vaccine; in fact, a similar sequence induces protection against the virus by producing IL-2.	[18, 22-23]
B 357-366	VGPVFPPGM	It was identified by functional mapping. This sequence corresponds to a restricted epitope (H-2 ^b), recognized by CD8 T cells, and is associated with the expression of CD107a / b and IFN- γ .	[17, 24-25]
C 376-384	PSREDNLQR	Region recognized by CD4 T cells (H-2 ^d) in mice, which is associated with the production of IL-2, TNF, and IFN- γ , although to a lesser extent than other regions of the protein. On the other hand, a similar region containing this sequence induces significant protection against viral shedding after intranasal immunization.	[15, 18, 26]

The simulation results showed that the temperature increase causes significant changes in the structure of some regions of VP6. As Fig. 1 shows, these changes are more evident in epitopes A and B, in which the majority of their amino acid residues form a turn-like structure (turn, T). On the other hand, epitope C is structurally more conserved since it is placed in an alpha helix-like structure.

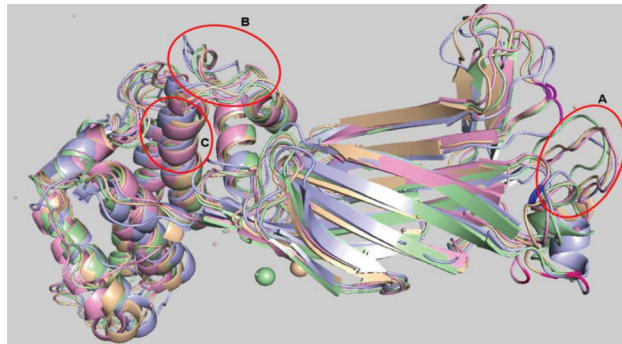


Figure 1: The VP6 secondary structure is modified as a result of temperature changes. The protein at 310 K is shown in blue, at 317 K in green, at 322 K in pink, and at 322 K with the simulation of an electric field in orange. The red circles show the location of the epitopes.

As the temperature rises, the system increases its kinetic energy, which is reflected in the random movement of some residues whose atoms vibrate, generating rotation and translation movements that are manifested to a greater extent in regions with a less steric deterrent. These movements modified the interatomic distances, forcing amino acid residues to be grouped into different secondary structures, even in ultra-short time intervals. In Fig. 2, we show a) the VP6 contact map, which is a bidimensional representation of the distances among all the residues. Dark areas imply that residues are at distances greater than 1.5 nm, while the lightest points represent those with distances less than 1.5 nm. b) VP6 secondary structure at 322 K during the first

1000 ps is conserved except in the region 301-308 that belongs to epitope A, which restructures from A-helix to turns (T).

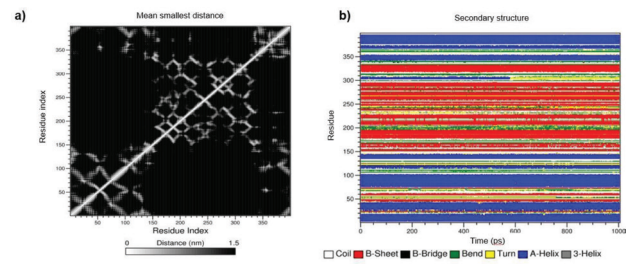


Figure 2: a) VP6 contact map. The dark areas imply that the residues are located at distances greater than 1.5 nm. The clearest points represent a pair of amino acid residues located at distances less than 1.5 nm. b) Secondary structure of VP6 at 322K during the first 1000 ps.

We calculated the root mean square fluctuations per VP6 residue for 310 K, 317 K, and 322 K temperatures; it can be observed that when the temperature decreases, the flexibility of the protein is increased in several regions of its structure (Fig. 3a). However, when applying an electric field, fluctuations decrease throughout the molecule (Fig. 3b), and particularly, in epitope C.

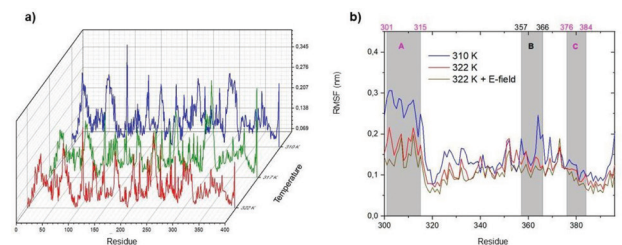


Figure 3: a) Root mean square fluctuations per VP6 amino acid residue for three temperatures. b) Comparison of residue fluctuations forming the epitopes A, B, and C. It is observed that the presence of the electric field mitigates the fluctuations in the region 300-396.

The charge distribution in a protein and, in particular, in its epitopes, is of great importance because it is closely related to protein-protein and protein-ligand interactions. It should be noted that it has been experimentally demonstrated that epitopes of VP6 have a high density of charged residues and that charge density is proportional to the number of antibodies that bind to them [27].

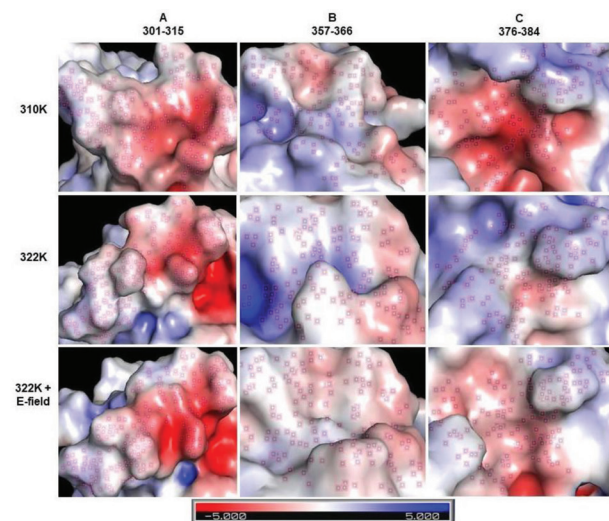


Figure 4: Charge distribution of epitopes in the VP6 region 300-396. The red boxes indicate the location of the atoms forming the amino acid residues of the epitopes.

In the specific case of the region 300-396, we analyzed the distribution of electric charge in epitopes A, B, and C by increasing the temperature from 310K to 322K. Subsequently; we incorporated the stimulus of an electric field in the 322 K system. As shown in Fig. 4, in epitope A, there are slight changes in the electric charge distribution when the temperature increases; this phenomenon is not accentuated by the application of the field. On the other hand, in the epitope B, the temperature increase causes a redistribution of electric charge until neutrality is reached in some areas, which becomes even more evident when incorporating the stimulus of the electric field. In the case of epitope C, an inversion of charge occurs (from negative to positive) as the temperature increased, but this effect is reversed when the electric field is applied. Thermoelectric effects are presented due to the conductive nature of VP6 (García-García *et al.*, 2019).

Conclusions

The *in silico* analysis showed that epitope A has a higher density of electrically charged residues and greater structural flexibility. However, its efficiency in attracting antibodies might be diminished because its residues, in the state of

minimum energy, are stable and located in an alpha helix structure; but as the temperature increases, in very short times (600 ps), the aforementioned conformation is lost, and the residues are reconfigured to form a turn structure. As a result, its antigenic determinant function might be compromised.

The charge distribution in epitopes A, B, and C agrees with that reported in experimental tests [21]. Furthermore, we can appreciate that the application of the field induces electrical neutrality in the epitope B; consequently, the affinity constant between VP6 and immunoglobulins might be reduced due to the increase of Van der Waals type interactions in detriment of Coulomb interactions. However, the fluctuations of the residues - induced by the electric field - decrease significantly in this region, which could facilitate the coordinated movement of their amino acid residues, as well as minimize the forces that restrict them to favor protein-ligand interactions.

With respect to epitope C, it was observed that it has a poorly flexible structure, and temperature changes did not affect this condition. Nonetheless, the temperature increase was sufficient to generate a thermoelectric effect that reversed the charge distribution - from negative to positive -, phenomenon that was partially reversed when the electric field was applied.

Acknowledgments

The authors thank CONCAEM and COPARMEX, State of Mexico, for the support received in the development of this project.

References

- [1] J. E. Tate et al., Clin Infect Dis. Dis. **62**, S96 (2016). <https://doi.org/10.1093/cid/civ1013>
- [2] M. K. Estes and H. B. Greenberg, in Fields Virology, edited by D. M. Knipe and P. M. Howley (Lippincott Williams & Wilkins, Philadelphia, 2013), 6th ed., 1347–1401.
- [3] R. L. Ward and M. M. McNeal, J. Infect. Dis. **202**, S101 (2010). <https://doi.org/10.1086/653556>
- [4] S. Lappalainen et al., Archives of virology **160**, 2075 (2015). <https://doi.org/10.1007/s00705-015-2461-8>
- [5] M. Mathieu et al., EMBO J **20**, 1485 (2001). <https://doi.org/10.1093/emboj/20.7.1485>
- [6] I. Erk et al., J. Virol. **77**, 3595 (2003). <https://doi.org/10.1128/JVI.77.6.3595-3601.2003>
- [7] T. Grant and N. Grigorieff, Elife **4**, e06980 (2015). <https://doi.org/10.7554/eLife.06980>

- [8] W. I. García-García et al., *Bioelectrochemistry* **127**, 180 (2019).
<https://doi.org/10.1016/j.bioelechem.2019.02.012>
- [9] K. F. Ready and M. Sabara, *Virology* **157**, 189 (1987).
[https://doi.org/10.1016/0042-6822\(87\)90328-X](https://doi.org/10.1016/0042-6822(87)90328-X)
- [10] J. Lepault et al., *EMBO J.* **20**, 1498 (2001).
<https://doi.org/10.1093/emboj/20.7.1498>
- [11] K. F. M. Ready, M. I. J. Sabara and L. A. Babiuk, *Virology* **167**, 269 (1988).
[https://doi.org/10.1016/0042-6822\(88\)90077-3](https://doi.org/10.1016/0042-6822(88)90077-3)
- [12] E. A. Mansell, R. F. Ramig and J. T. Patron, *Virology* **204**, 69 (1994).
<https://doi.org/10.1006/viro.1994.1511>
- [13] M. Munoz, M. Rios and E. Spencer, *Intervirology* **38**, 256 (1995). <https://doi.org/10.1159/000150448>
- [14] G. Tosser et al., *J. Virol.* **66**, 5825 (1992).
- [15] A. H. Choi et al., *Vaccine* **21**, 761 (2003).
[https://doi.org/10.1016/S0264-410X\(02\)00595-9](https://doi.org/10.1016/S0264-410X(02)00595-9)
- [16] M. M. McNeal et al., *Virology* **363**, 410 (2007).
<https://doi.org/10.1016/j.virol.2007.01.041>
- [17] M. A. Franco et al., *J. Gen. Virol* **75**, 589 (1994).
<https://doi.org/10.1099/0022-1317-75-3-589>
- [18] W. Zhao, B. Pahar and K. Sestak, *Virology: research and treatment* **1**, 9 (2008).
<https://doi.org/10.4137/VRT.S563>
- [19] B. Winter and M. Faubel, *Chem. Rev.* **106**, 1176 (2006). <https://doi.org/10.1021/cr040381p>
- [20] S. A. Egorov, K. F. Everitt and J. L. Skinner, *J. Phys. Chem. A* **103**, 9494 (1999).
<https://doi.org/10.1021/jp9919314>
- [21] D. R. Hekstra et al., *Nature* **540**, 400 (2016).
<https://doi.org/10.1038/nature20571>
- [22] M. Parra et al., *Virology* **191**, 452–453 (2014).
<https://doi.org/10.1016/j.virol.2014.01.014>
- [23] O. V. Morozova et al., *Virus genes* **54**, 225 (2018). <https://doi.org/10.1007/s11262-017-1529-9>
- [24] M. C. Jaimes, N. Feng and H. B. Greenberg, *J virol* **79**, 4568 (2005).
<https://doi.org/10.1128/JVI.79.8.4568-4579.2005>
- [25] J. Q. Jiang et al., *J virol* **82**, 6812 (2008).
<https://doi.org/10.1128/JVI.00450-08>
- [26] A. H. C. Choi et al., *J virol* **74**, 11574 (2000).
<https://doi.org/10.1128/JVI.74.24.11574-11580.2000>
- [27] M. S. Aiyegbo et al., *PLoS ONE* **8**, e61101 (2013).
<https://doi.org/10.1371/journal.pone.0061101>



Journal of Nuclear Physics, Material Sciences, Radiation and Applications

Chitkara University, Saraswati Kendra, SCO 160-161, Sector 9-C,
Chandigarh, 160009, India

Volume 7, Issue 2

February 2020

ISSN 2321-8649

Copyright: [© 2020 D. Osorio-González et al.] This is an Open Access article published in Journal of Nuclear Physics, Material Sciences, Radiation and Applications (J. Nucl. Phys. Mat. Sci. Rad. A.) by Chitkara University Publications. It is published with a Creative Commons Attribution- CC-BY 4.0 International License. This license permits unrestricted use, distribution, and reproduction in any medium, provided the original author and source are credited.
